Formation of the metal-oxide nanocomposites during the partial reduction of Nd-Sr nickelates

Sergey A. Malyshev[1,2,a], Oleg A. Shlyakhtin[1,b], Grigorii M. Timofeev[1,c], Galina N. Mazo[1,d], Ilya V. Roslyakov[3,4,e], Aleksander V. Vasiliev[1,f], Tatiana B. Shatalova[1,g], Aleksander L. Kustov[1,h]

[1]Department of Chemistry, M. V. Lomonosov Moscow State University, 119991 Moscow, Russia

[2]Department of Materials Sciences, Shenzhen MSU-BIT University, Shenzhen 518172, China

[3]Department of Materials Sciences, M. V. Lomonosov Moscow State University, 119991 Moscow, Russia

[4]N. S. Kurnakov Institute of General and Inorganic Chemistry, Russian Academy of Sciences, 119991 Moscow, Russia

[a]malyshev12sa@yandex.ru, [b]oleg@inorg.chem.msu.ru, [c]timofeevg@inbox.ru, [d]mazo@inorg.chem.msu.ru, [e]Ilya.roslyakov@gmail.com, [f]a.vasiliev@inorg.chem.msu.ru, [g]shatalovatb@gmail.com, [h]kyst@list.ru

Corresponding author: O. A. Shlyakhtin, oleg@inorg.chem.msu.ru

ABSTRACT A thermal reduction of $Nd_{2-x}Sr_xNiO_{4-\delta}$ ($x = 0$–1.4) solid solutions in an Ar/H_2 gas mixture occurs in several separate stages. The initial stages of reduction presumably related to the reduction of Ni^{3+} to Ni^{2+} cause only minor changes in the initial K_2NiF_4 type structure and retain the morphology of the complex oxide particles. Occasionally, this process is accompanied by the appearance of Ni metal nanoparticles at the surface of oxide grains. As-obtained Ni/metal oxide nanocomposites similar to the products of redox exsolution demonstrate noticeable catalytic activity in the reaction of CO_2 hydrogenation at T = 350–400°C.

KEYWORDS nanoparticles, nanocomposites, thermal reduction, redox exsolution, catalysis, CO_2 hydrogenation.

1. Introduction

Most of the modern chemical synthesis methods of metal-oxide nanocomposites are based on the soaking of refractory substrates with solutions containing transition metals followed by the thermal reduction of the dried substrate [1]. However, the growing attention has been attracted in recent years by the new synthesis techniques based on the formation of metal-oxide nanocomposites in situ, by the thermal decomposition of solid multicomponent precursors in the reductive environment. Along with polynuclear complex compounds and metal-organic frameworks (MOF), complex oxides of transition elements could be also used as precursors in this synthesis [2–4].

An original synthesis technique was proposed last years based on the partial reduction of several complex oxides at elevated temperatures in the reducing environment. Despite retaining the crystal structure of the initial complex oxide with minor changes only, this process is accompanied by the formation of the isolated spherical nanoparticles of the transition or noble metals at the surface of larger grains of the precursor compound [5–7]. An essential feature of nanocomposites obtained by this technique called redox exsolution is their enhanced thermal stability due to socketing the metal particles to the surface of precursor grains. This effect was observed for a limited number of rather specific complex oxides like cation-deficient perovskites or solid solutions containing a small amount of transition metals only [8–10]. Due to the low rate of metal particle formation, this process usually takes processing for several hours at elevated temperatures, usually at T > 700°C.

Recent studies demonstrated that metal-oxide nanocomposites with morphology rather similar to the products of redox exsolution could be obtained by the complete thermal reduction of complex oxides of rare earth, cobalt, and nickel with K_2NiF_4 structure [11–13]. Another feature of these nanocomposites that makes them similar to the redox exsolution products is their excellent catalytic activity, selectivity, and stability of the catalytic properties in the processes of partial oxidation and dry reforming of methane at T = 750–850°C.

During these studies, it was found that complex oxides $Nd_{2-x}Sr_xNiO_{4-\delta}$ with K_2NiF_4 structure used as precursors could be obtained for $x \leq 1.4$ though the formation of these compounds is rather complicated; some of them could be obtained at $T > 1100°C$ only [14]. A complete reduction of these compounds is usually completed at $T > 800°C$; this temperature usually increases with an increase in Sr content. All these processes are realized in two distinct stages.

The first step of this process has never been studied before. Taking into account an expected similarity of this stage – partial reduction of $Nd_{2-x}Sr_xNiO_{4-\delta}$ – with redox exsolution processes and, hence, the possibility to observe the formation of Ni nanoparticles at the surface of partial reduction products, the present study was aimed at the investigation of the processes and products of the partial reduction of $Nd_{2-x}Sr_xNiO_{4-\delta}$. Due to the limited thermal stability of these products, the evaluation of their catalytic properties was performed in the CO_2 hydrogenation process usually realized at 300–400°C [15–18].

2. Experimental

A series of complex oxide precursors $Nd_{2-x}Sr_xNiO_{4-\delta}$ ($x = 0$; 0.5; 1; 1.2; 1.4) was obtained by the freeze drying synthesis method. The details of the synthesis technique can be found elsewhere [14]. Briefly, the aqueous solutions of Nd nitrate, Ni nitrate, and Sr acetate taken in the stoichiometric ratio were mixed with an aqueous solution of polyvinyl alcohol (5 mass. %) to avoid melting during freeze drying. As-obtained solutions with different x values were flash-frozen by liquid nitrogen and freeze dried at P = 0.7 mbar for 2 days. According to the results of previous studies [14], thermal processing of freeze dried precursors was performed in air at T = 1200°C for 6 h to ensure the complete phase formation of all K_2NiF_4-like solid solutions in this series. A reduction of these complex oxides was performed in 10% H_2/Ar gas mixture at different temperatures for 1 h followed by slow cooling in Ar/H_2 stream to room temperature.

XRD analysis of precursors and their reduction products was implemented with a Rigaku D/MAX-2500PC diffractometer (Rigaku, Tokyo, Japan) with Cu $K_{\alpha1,2}$ radiation generated on a rotating Cu anode (40 kV, 250 mA). The profile analysis of the powder XRD data was carried out by the Le Bail method using the Jana 2006 program package. The TG-DSC thermal analysis of samples was performed in a 10% H_2/Ar gas mixture by STA 409PC/PG (NETZSCH) at T = 40°C – 1000°C and a 5°C/min heating rate. The morphology of the powders was studied using a Carl Zeiss NVision 40 scanning electron microscope (Carl Zeiss SMT AG, Oberkochen, Germany). The magnetic properties were studied using the Faraday balance magnetometer at room temperature. The instrumentation was manufactured at the Institute of Solid-State Chemistry of the Ural Branch of the Russian Academy of Sciences. The magnetic field varied from -17.9 to 17.9 kOe. The relative error in determining the magnetization was 3%. The error in determining the coercive force was ±100 Oe.

The catalytic properties of the partial reduction products in a CO_2 hydrogenation were studied in a flow-through catalytic apparatus equipped with a stainless steel reactor (4 mm inner diameter) with a fixed catalyst bed. The catalyst sample (200 mg of a catalyst and mixed with quartz glass powder in a 1:2.5 mass ratio) in the form of 0.25–0.5 mm particles was placed in a vertically placed reactor. Hydrogen and carbon dioxide were fed by Bronkhorst EL-FLOW Prestige flow controllers in H_2/CO_2 = 2/1 gas mixture at atmospheric pressure in the absence of dilution with inert gas at 250–400°C at the total reaction mixture flow rate of 100 ml/min.

The total CO_2 conversion (X, %) was calculated from the carbon dioxide loss:

$$x = \left(\frac{G^0 X^0_{CO_2} - GX_{CO_2}}{G^0 X^0_{CO_2}} \right) \cdot 100\%,$$

where $X^0_{CO_2}$ and X_{CO_2} are fractions of carbon dioxide before and after the reactor, and $G^0 X^0_{CO_2}$ and GX_{CO_2} are the carbon dioxide gas flows before and after the reactor.

The product selectivity (S, %) was determined by the equation:

$$S_i = \left(\frac{X_i}{\sum X} \right) \times 100\%,$$

The CO_2 performance was calculated using the equation:

$$P = \frac{G^0 X^0_{CO_2} - GX_{CO_2}}{m_{cat}},$$

where m_{cat} is the catalyst mass.

3. Results and discussion

According to the results of previous studies, all $Nd_{2-x}Sr_xNiO_{4-\delta}$ complex oxides with K_2NiF_4 structure belong to the space group I4/mmm except Nd_2NiO_4 ($x = 0$) belonging to the space group Fmmm [14]. A complex dependence of lattice parameters during the substitution of Nd with Sr in these solid solutions could be explained by the interplay of the difference in ionic radii of Nd^{3+} and Sr^{2+}, different ratio Ni^{3+}/Ni^{2+} and rather different oxygen stoichiometry in these complex oxides. However, the temperature of thermal reduction of these compounds in an H_2/Ar gas mixture resulted in the formation of Ni metal, Nd_2O_3, and SrO demonstrates a systematic increase with the growing amount of strontium

in their composition [14]. The precise oxygen stoichiometry of Nd_2O_3 and SrO allows one to use the total mass change during this reduction for a rather exact evaluation of the oxygen stoichiometry in $Nd_{2-x}Sr_xNiO_{4-\delta}$.
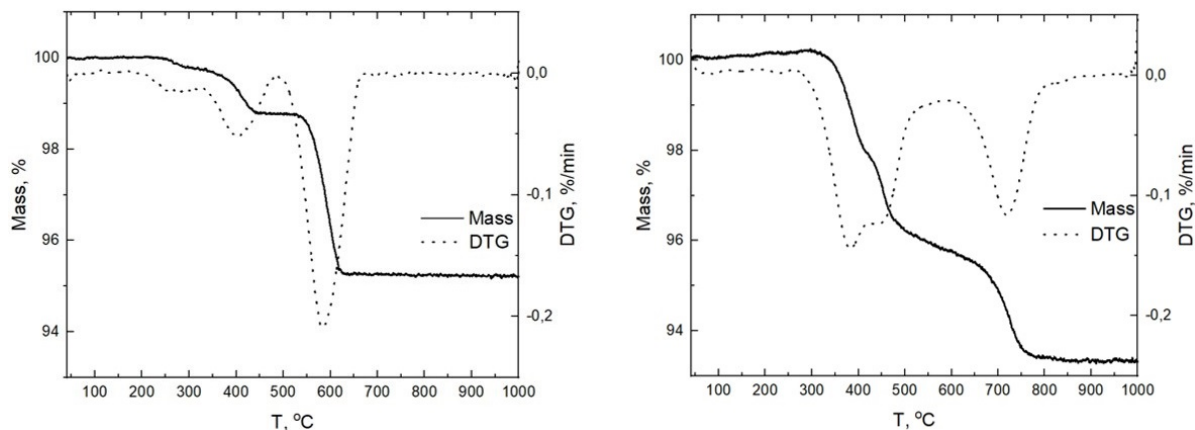

FIG. 1. TG and DTG curves of the reduction of Nd_2NiO_4 ($x = 0$) and $NdSrNiO_{4-\delta}$ ($x = 1$) in the 10% H_2/Ar gas mixture

Another essential feature of these thermal reduction processes deals with their multistage character in all these products (Fig. 1). The mass loss ratio of the first to last steps in TG increases with x. Taking into account that the substitution of Nd with Sr in Nd_2NiO_4 causes a systematic increase of Ni oxidation state from Ni^{2+} to Ni^{3+}, the first stages of the thermal reduction could be affiliated with the reduction of Ni^{3+} to Ni^{2+}.

To study the products of these stages in more detail, the products of the partial reduction of $Nd_{2-x}Sr_xNiO_{4-\delta}$ for $x = 0$–1.4 were obtained by the isothermal treatment of initial complex oxides in Ar/H_2 at T = 500°C, just before the beginning of the last stage of reduction. Analysis of their XRD patterns (Fig. 2, Supplementary, Fig. S1,S2) demonstrated the formation of the new individual complex oxides; their lattice parameters are given in Table 1. The partial reduction product of Nd_2NiO_4 belongs to orthorhombic space group Aema while in other cases the reduced complex oxides belong to Immm structure. A small amount of Nd_2O_3 in this sample could be attributed to the beginning of the second stage of reduction of Nd_2NiO_4 (Fig. 2 ($x = 0$), Fig. S1).
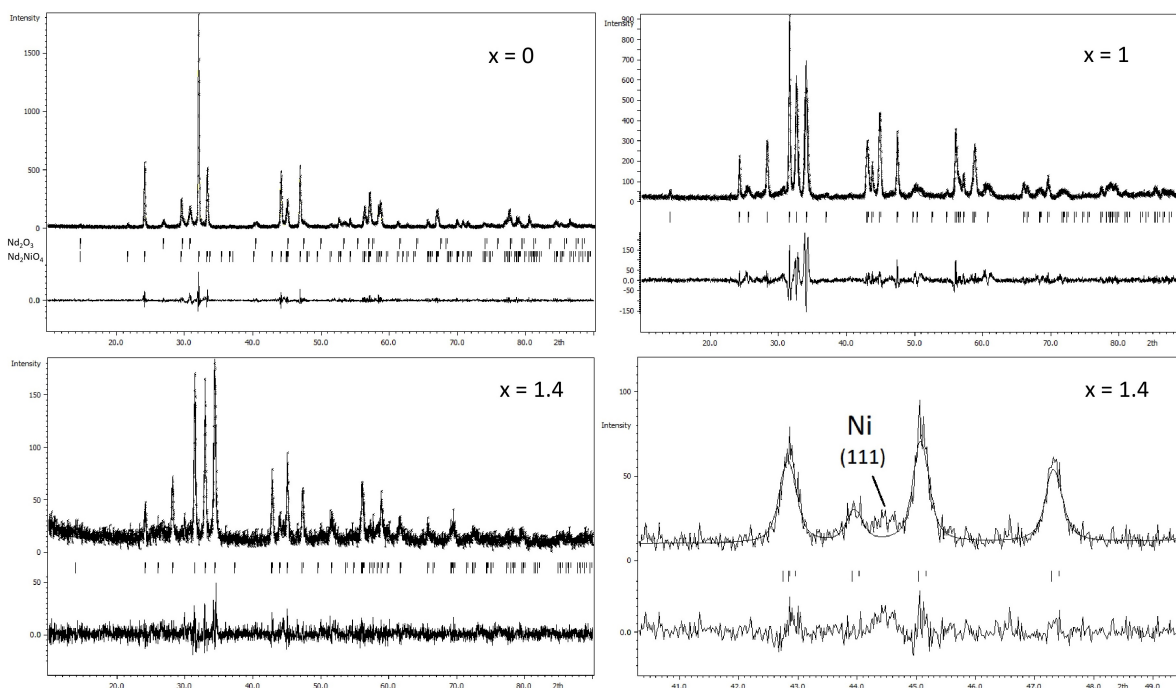

FIG. 2. Le Bail profile refinement plots of the partial reduction products of $Nd_{2-x}Sr_xNiO_{4-\delta} - (x = 0, 1$ and 1.4) at 500°C

A comparison of these data with the lattice parameters of the corresponding precursor compounds described in [14] shows that the minimal changes in lattice volume are observed for Nd_2NiO_4 ($x = 0$) and $Nd_{1.5}Sr_{0.5}NiO_{4-\delta}$ ($x = 0.5$),

TABLE 1. Lattice parameters of the partial reduction products of $Nd_{2-x}Sr_xNiO_{4-\delta}$

Sample	Space group	a, Å	b, Å	c, Å	V, Å
$x = 0$	Aema	5.8335(5)	5.3830(4)	12.119(18)	364.24(6)
$x = 0.5$	Immm	3.7114(2)	3.8232(2)	12.501(17)	177.40(3)
$x = 1$	Immm	3.622(19)	3.8303(5)	12.591(2)	174.68(5)
$x = 1.2$	Immm	3.5503(4)	3.8324(3)	12.665(17)	172.33(4)
$x = 1.4$	Immm	3.538(18)	3.835(18)	12.630(3)	171.38(8)

where the amount of Ni^{3+} and, hence, the intensity of reduction processes were rather small. For complex oxides with $x \geq 1$, the volume is changed more significantly which indicates a difference in the topochemical mechanisms of reduction processes. This difference could be attributed both to a larger amount of Ni^{3+} in the precursor oxide and/or to a more significant effect of strontium with its rather specific chemistry of high temperature processes. Another intriguing feature observed in the XRD pattern of $Nd_{0.6}Sr_{1.4}NiO_{4-\delta}$ reduction product is a small peak attributed to Ni^0 metal that was not identified in other samples.

Analysis of the morphology of the partial reduction products demonstrated retaining the initial morphology of precursor powders with their large micron-sized crystallites formed during their synthesis at 1200°C (Fig. 3). The most important feature of these micrographs is that there is a large number of tiny nanospheres at the surface of large grains of oxide reduction products with $x = 0.5$, 1, and 1.2. It is worth noting, that the sample with $x = 1.2$ is characterized by a slightly larger average particle diameter along with significantly increased size distribution width (Fig. 3F).
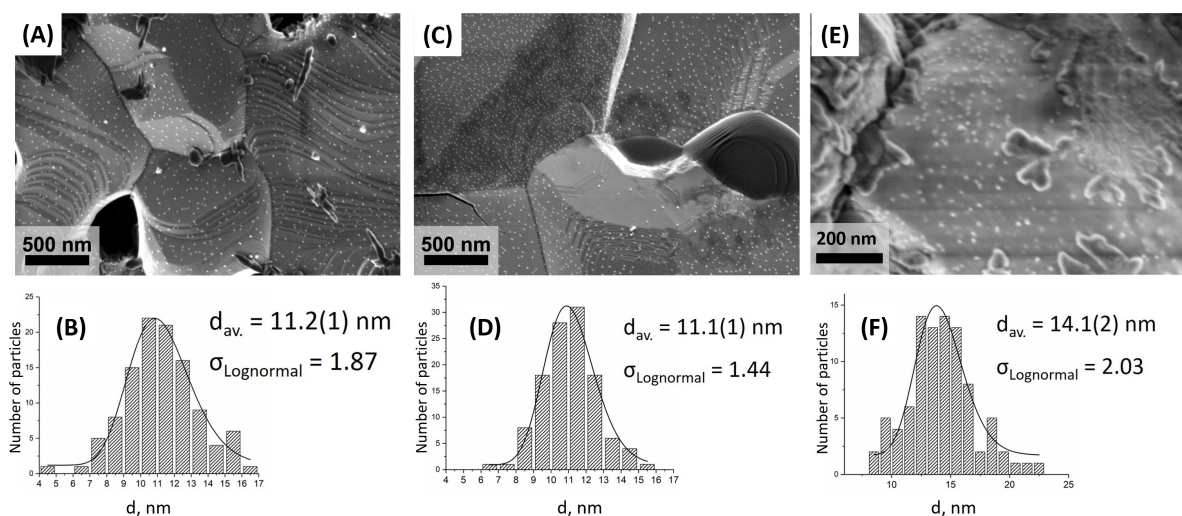

FIG. 3. SEM micrographs of the partial reduction products of $Nd_{2-x}Sr_xNiO_{4-\delta}$ at 500°C for $x = 0.5$ (A,B), $x = 1$ (C,D) and $x = 1.4$ (E,F)

Similar spherical nanoparticles have been observed before during previous studies of $(R,Ca)_2(Co,Ni)O_4$ reduction products [11–14] but they were observed in the products of complete reduction only and have been identified as nanoparticles of Ni metal being one of the main natural products of the complete reduction. The appearance of Ni metal in the products of partial reduction of $Nd_{2-x}Sr_xNiO_{4-\delta}$ affiliated with a reduction of Ni^{3+} to Ni^{2+} and accompanied by the minor changes of the initial K_2NiF_4 structure looks rather unusual.

It should be mentioned, however, that similar particles have been also observed during another partial reduction process that occurred in other complex oxides at much higher temperatures, during redox exsolution [7–10]. Hence, it is rather probable that the nanoparticles observed in Fig. 3 belong to the nickel metal too. Taking into account that the Ni metal is the only ferromagnetic among possible reaction products, the appearance of nickel at the early stages of $Nd_{2-x}Sr_xNiO_{4-\delta}$ reduction was confirmed by the results of magnetic measurements. The observed magnetization curves usual for the soft ferromagnetic materials clearly confirmed the appearance of a significant amount (several mass. %) of magnetic phase in all products of partial reduction in the study (Fig. 4) while the initial compounds demonstrated the common paramagnetic behavior.
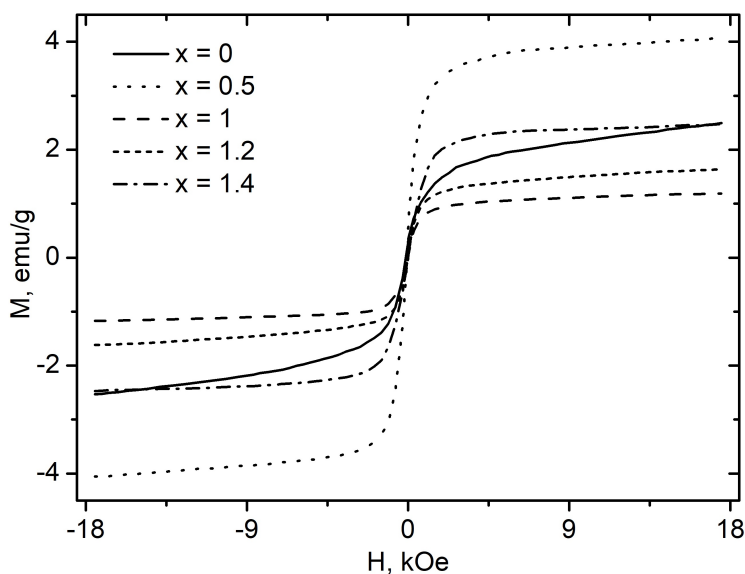
FIG. 4. Magnetization curves of the partial reduction products of $Nd_{2-x}Sr_xNiO_{4-\delta}$

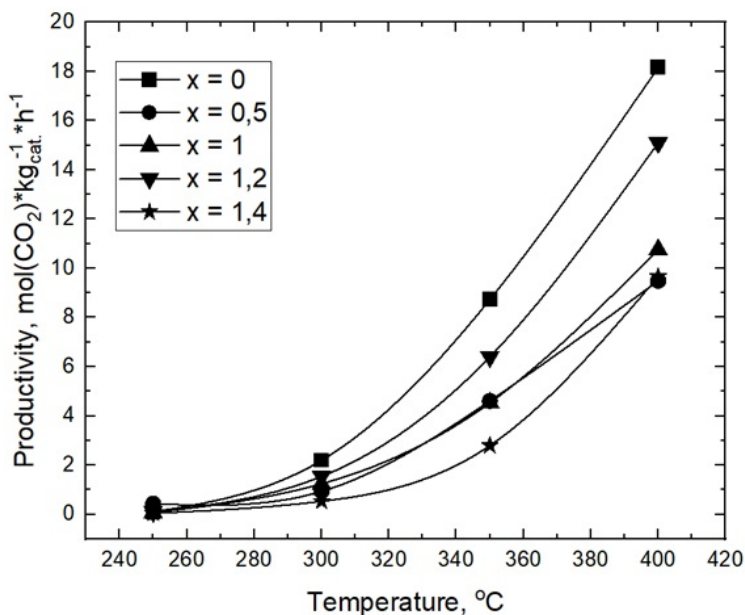FIG. 5. The productivity of the partial reduction products of $Nd_{2-x}Sr_xNiO_{4-\delta}$ as catalysts of CO_2 hydrogenation at various temperatures

The amount of magnetic phase in these samples is rather different and doesn't demonstrate any obvious correlations with the composition of the precursor compound. This feature clearly indicates that several different topochemical processes could occur during the partial reduction of complex oxides. One of them deals with a soft transformation of the crystal lattice of precursor compound caused by the reduction of Ni^{3+} to Ni^{2+}. Another process involves a more intensive reduction of Ni^{3+} to Ni^0. The ratio between these two reaction pathways could depend on several factors that are not clear right now, and more detailed mechanistic studies are needed to control the nanoparticle formation process.

Despite these obstacles, this interesting process could be used right now as one more synthesis technique to obtain functional metal-oxide nanocomposites. To demonstrate the potential usefulness of these materials, their catalytic properties have been evaluated in the reaction of CO_2 hydrogenation usually occurring at T = 300–400°C. All the materials in the study demonstrated a significant catalytic activity usual for Ni-based catalysts (Fig. 5); the main reduction products are CO and CH_4 (Supplementary, Table S1). The highest catalytic activity is demonstrated by the Sr-free partial reduction product of Nd_2NiO_4 which could be associated with the smallest size of Ni nanoparticles in this composite. A correlation of catalytic activity of other composites with x, amount of magnetic particles, or their size doesn't look obvious that could

be caused by the different reduction mechanisms of different precursor compounds and different spatial distribution of Ni nanoparticles inside the particles of reduction product.

Finally, we have to note that the processes of metal nanoparticles during the partial reduction of complex nickelates have been observed for the first time in the present study. These processes occur simultaneously with a soft transformation of the crystal lattice of matrix oxide at the first stages of reduction. Apart from another kind of partial reduction processes, redox exsolution, these processes occur in a short time at rather moderate temperatures. The complex character of these processes deserves more detailed study by modern instrumental methods. The potential practical usefulness of these processes for materials synthesis could be confirmed by the significant catalytic activity of Ni-based metal-oxide nanocomposites obtained by this method.

References

[1] Ray C., Pal T. Recent advances of metal-metal oxide nanocomposites and their tailored nanostructures in numerous catalytic applications. *J. Mater. Chem. A*, 2017, **5**, P. 9465–9487.

[2] Zhou L.X., Yang Y.Y., Zhu H.L., Zheng Y.Q. In situ synthesis of Ag/NiO derived from hetero-metallic MOF for supercapacitor application. *Chem Papers*, 2021, **75**, P. 1795–1807.

[3] Konnerth H., Matsagar B.M., Chen S.S., Prechtl M.H.G., Shieh F.K., Wu K.C.W. Metal-organic framework (MOF)-derived catalysts for fine chemical production. *Coord. Chem. Rev*, 2020, **416**, P. 213319.

[4] Bhattar S., Abedin M.A., Kanitkar S., Spivey J.J. A review on dry reforming of methane over perovskite derived catalysts. *Catal.Today*, 2021, **365**, P. 2–23.

[5] Kwon O., Joo S., Choi S., Sengodan S., Kim G. Review on exsolution and its driving forces in perovskites. *J. Phys. Energy*, 2020, **2**, P. 032001.

[6] Fan W., Sun Z., Bai Y. Manipulating Electrocatalytic Activity of Perovskite Oxide Through Electrochemical Treatment, *Small*, 2022, **18**, P. 2107131.

[7] Neagu D., Tsekouras G., Miller D.N., Mernard H., Irvine J.T.S. In situ growth of nanoparticles through control of non-stoichiometry. *Nature Chem.*, 2013, **5**, P. 916–923.

[8] Han H., Park J., Nam S.Y., Kim K.J., Choi G.M., Parkin S.S.P., Jang H.M., Irvine J.T.S. Lattice strain-enhanced exsolution of nanoparticles in thin films. *Nature Comm.*, 2019, **10**, P. 1471.

[9] Shah S., Sayono S., Ynzunza J., Pan R., Xu M., Pan X., Gilliard-AbdulAziz K.L. The effects of stoichiometry on the properties of exsolved Ni-Fe alloy nanoparticles for dry methane reforming. *AIChE J.*, 2020, **66**, P. e17078.

[10] Gao Y., Chen D., Saccoccio M., Lu Z., Ciucci F. From material design to mechanism study: Nanoscale Ni exsolution on a highly active A-site deficient anode material for solid oxide fuel cells. *Nano Energy*, 2016, **27**, P. 499–508.

[11] Shlyakhtin O.A., Malyshev S.A., Loktev A.S., Mazo G.N., Garshev A.V., Chumakov R.G., Dedov A.G. Synthesis and Decomposition of $Nd_{2-y}Ca_yCo_{1-x}Ni_xO_4$: The Effect of Resynthesis on the Catalytic Performance of Decomposition Products in the Partial Oxidation of Methane. *ACS Appl. Energy Mater.*, 2021, **4**(8), P. 7661–7673.

[12] Malyshev S.A., Shlyakhtin O.A., Loktev A.S., Mazo G.N., Timofeev G.M., Mukhin I.E., Kaplin I.Yu., Svetogorov R.D., Valeev R.G., Dedov A.G. Exsolution-like synthesis of Ni/(Nd$_2$O$_3$,CaO) nanocomposites from $Nd_{2-x}Ca_xNiO_4$ precursors for catalytic applications. *J. Solid State Chem.*, 2022, **312**, P. 123267.

[13] Malyshev S.A., Shlyakhtin O.A., Loktev A.S., Mazo G.N., Timofeev G.M., Mukhin I.E., Svetogorov R.D., Roslyakov I.V., Dedov A.G., Ni/(R$_2$O$_3$,CaO) Nanocomposites Produced by the Exsolution of $R_{1.5}Ca_{0.5}NiO_4$ Nickelates (R = Nd, Sm, Eu): Rare Earth Effect on the Catalytic Performance in the Dry Reforming and Partial Oxidation of Methane. *Materials*, 2022, **15**, P. 7265(1-11).

[14] Shlyakhtin O.A., Timofeev G.M., Malyshev S.A., Loktev A.S., Mazo G.N., Shatalova T.B., Arkhipova V.A., Roslyakov I.V., Dedov A.G., $Nd_{2-x}Sr_xNiO_4$ solid solutions: synthesis, structure and enhanced catalytic properties of their reduction products in the dry reforming of methane, *Catalysts*, 2023, **13**, P. 966.

[15] Stangeland K., Kalai D., Li H., Yu Z. The effect of temperature and initial methane concentration on carbon dioxide methanation on Ni based catalysts. *Energy Procedia*, 2017, **105**, P. 2016–2021.

[16] Zhang T., Liu Q. Perovskite LaNiO3 Nanocrystals inside Mesostructured Cellular Foam Silica: High Catalytic Activity and Stability for CO$_2$ Methanation. *Energy Technol.*, 2020, **8**, P. 1901164.

[17] Evdokimenko N., Ermekova Zh., Roslyakov S., Tkachenko O., Kapustin G., Bindiug D., Kustov A., Mukasyan A.S. Sponge-like CoNi Catalysts Synthesized by Combustion of Reactive Solutions: Stability and Performance for CO$_2$ Hydrogenation. *Materials*, 2022, **15**, P. 5129.

[18] Vikanova K.V., Kustov A.L., Makhov E.A., Tkachenko O.P., Kapustin G.I., Kalmykov K.B., Mishin I.V., Nissenbaum V.D., Dunaev S.F., Kustov L.M. Rhenium-contained catalysts based on superacid ZrO$_2$ supports for CO$_2$ utilization. *Fuel*, 2023, **351**, P. 128956.

Information about the authors:

Sergey A. Malyshev – Department of Materials Sciences, Shenzhen MSU-BIT University, Shenzhen 518172, China; Department of Chemistry, M. V. Lomonosov Moscow State University, 119991 Moscow, Russia; ORCID 0009-0005-0132-4466; malyshev12sa@yandex.ru

Oleg A. Shlyakhtin – Department of Chemistry, M. V. Lomonosov Moscow State University, 119991 Moscow, Russia; ORCID 0000-0001-8362-1002; oleg@inorg.chem.msu.ru

Grigorii M. Timofeev – Department of Chemistry, M. V. Lomonosov Moscow State University, 119991 Moscow, Russia; ORCID 0009-0002-4855-7935; timofeevg@inbox.ru

Galina N. Mazo – Department of Chemistry, M. V. Lomonosov Moscow State University, 119991 Moscow, Russia; ORCID 0000-0001-7036-5927; mazo@inorg.chem.msu.ru

Ilya V. Roslyakov – N. S. Kurnakov Institute of General and Inorganic Chemistry, Russian Academy of Sciences, 119991 Moscow, Russia; Department of Materials Sciences, M. V. Lomonosov Moscow State University, 119991 Moscow, Russia; ORCID 0000-0002-9958-6659; Ilya.roslyakov@gmail.com

Aleksander V. Vasiliev – Department of Chemistry, M. V. Lomonosov Moscow State University, 119991 Moscow, Russia; ORCID 0000-0003-4108-9040; a.vasiliev@inorg.chem.msu.ru

Tatiana B. Shatalova – Department of Chemistry, M. V. Lomonosov Moscow State University, 119991 Moscow, Russia; ORCID 0000-0002-4304-8624; shatalovatb@gmail.com

Aleksander L. Kustov – Department of Chemistry, M. V. Lomonosov Moscow State University, 119991 Moscow, Russia; ORCID 0000-0003-0869-8784; kyst@list.ru